Fluorescently-Tagged Magnetic Protein Nanoparticles for High-Resolution Optical and Ultra-High Field Magnetic Resonance Dual-Modal Cerebral Angiography

Sandeep K. Mishra[*, 1,2], Peter Herman [1,2], Michael Crair[4], R. Todd Constable[1,5], John J. Walsh[3], Adil Akif[3], Justus V. Verhagen[4,6], Fahmeed Hyder[*1,2,3]

[1]Department of Radiology and Biomedical Imaging, [2]Magnetic Resonance Research Center, [3]Department of Biomedical Engineering, [4]Department of Neuroscience, [5]Department of Neurosurgery, Yale University, New Haven, CT, United States, [6]The John B. Pierce Laboratory, New Haven, CT, United States.

Correspondence:

*Sandeep Kumar Mishra/Fahmeed Hyder

The Anlyan Center (TAC), MRRC, 300 Cedar Street,

Yale University, New Haven, CT 06520, USA

Email: sandeepkmishra11@gmail.com/sandeep.kumar@yale.edu/fahmeed.hyder@yale.edu

Keywords: Extremely small iron oxide nanoparticles; T1/positive MRI; optical angiography; magnetic resonance angiography; cerebral angiography; magnetic protein nanoparticles.

Contents of Supplementary Materials.

Supplementary Table.

Table ST1. Magnetic Properties of NPs measured by SQUID at 1.5T applied magnetic field.

Supplementary Figures.

Fig. S1. EDX spectra of NPs showing elemental distributions.

Fig. S2. FTIR spectra of NPs as well as some intermediates.

Fig. S3. Colloidal stability of f-MPNPs.

Fig. S4. CIE fluorescent plot of fluorescent dye with and without conjugation.

Fig. S5. Photostability of f-MPNPs.

Fig. S6. XPS survey spectra c-FeMNPs and MPNPs.

Fig. S7. Evaluation of MRI properties of GdDOTA.

Fig. S8. Blood half-life of NPs based on fluorescent intensity and iron content in plasma.

Fig. S9. Cerebral angiography by real-time in vivo MRA of rats.

Fig S10. Cerebral angiography by real-time in vivo fluorescence imaging of rats.

Fig. S11. Biodistribution pattern for 3h and 24 h after i.v. injection of the f-MPNPs in rats.

Supplementary Movies.

Movie SM1. In vitro evaluation of concentration required for T1 MRI and optical imaging of large and small vessels phantom with different concentrations of f-MPNPs.

Movie SM2. In vivo 3D TOF MRA of mice brain pre- and post-injection of f-MPNPs.

Movie SM3. In vivo 3D FLASH MRA of mice brain at 0 min (pre-injection), and 5 min and 50 min post-injection of f-MPNPs.

Table ST1. Magnetic Properties of NPs measured by SQUID at 1.5T applied magnetic field.

	Magnetic moment (emu/g)	Coercivity (Oe)	Retentivity (emu/g)
c-FeMNPs	0.135	34.62	9.4×10^{-4}
f-MPNPs	0.085	26.51	11.2×10^{-4}

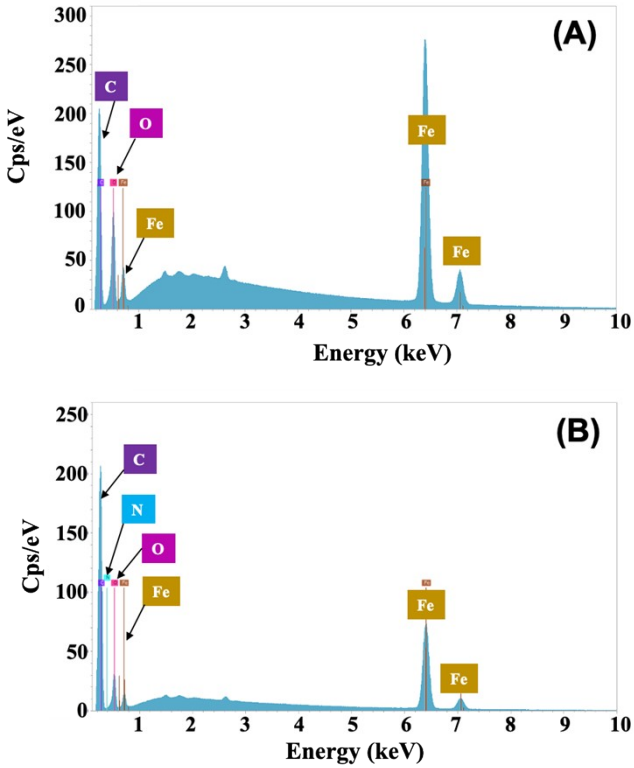

Figure S1. **EDX survey spectra of** magnetic NPs showing elemental distributions. **(A)** c-FeMNPs and **(B)** f-MPNPs.

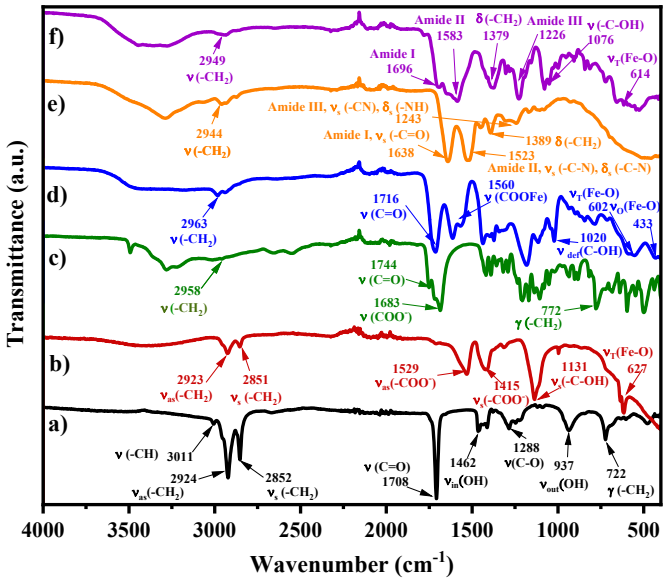

Figure S2. **FTIR spectra** of MNPs as well as some intermediates (with glossary of terms: **ν** = Stretching vibration; **δ** = Bending vibration; **γ** = Wagging, twisting, rocking; **def** = Deformation; **as** = Asymmetric; **s** = Symmetric).

a) Pristine oleic acid; -CH_2 asymmetric stretching vibration at 2924 cm^{-1} and symmetric vibration at 2852 cm^{-1}, and stretching vibration of C=O (of prominent -COOH group), and in-plane stretching vibration of –OH at 1462 cm^{-1} and out-plane stretching vibration of –OH at 1462 cm^{-1} are characteristic peaks of oleic acid. **b)** o-FeMNPs; after several washes and centrifugation to ensure excess oleic acid and oleyl alcohol are removed, the FTIR spectrum of oleic acid coated FeMNPs (o-FeMNPs) reveals additional peaks of $–COO^-$ asymmetric stretching vibration at 2924 cm^{-1} and symmetric vibration at 2852 cm^{-1}, and high intensity symmetric vibration of -C-OH, and symmetric vibration for tetragonal Fe-O confirming oleic acid coating on the surface of FeMNPs. **c)** Pristine sodium citrate; stretching vibration (-C=O) at 1744 cm^{-1}, and stretching vibration (-COO^-) at 1683 cm^{-1}, and rocking vibration (-CH_2) are characteristic peaks of sodium citrate. **d)** c-FeMNPs; citric acid coated FeMNPs reveals shift in stretching vibration (-C=O) to 1716 cm^{-1}, and shift in stretching vibration of (-COO^-) to 1560 cm^{-1} after interaction with Fe(III) ions on the nanoparticle surface. Appearance of additional peaks deformation vibration of (-C-OH), stretching vibration of tetrahedral Fe-O at 602 cm^{-1} and octahedral Fe-O at 433 cm^{-1} confirms citric acid surface modification on FeMNPs devoid of free citrate. **e)** Pristine bovine serum albumin (the model protein); characteristic peaks of the protein are Amide I at 1638 cm^{-1}, Amide II at 1523 cm^{-1} and Amide III at 1243 cm^{-1}. **f)** MPNPs; protein conjugation with c-FeMNPs shows shift in Amide I to 1696 cm^{-1}, Amide II to 1583 cm^{-1} and Amide III to 1226 cm^{-1}, and additional peaks of stretching vibration (C-OH) at 1076 cm^{-1} and of stretching vibration of tetrahedral Fe-O peak at 614 cm^{-1} confirm the covalent conjugation of c-FeMNPs and protein molecules.

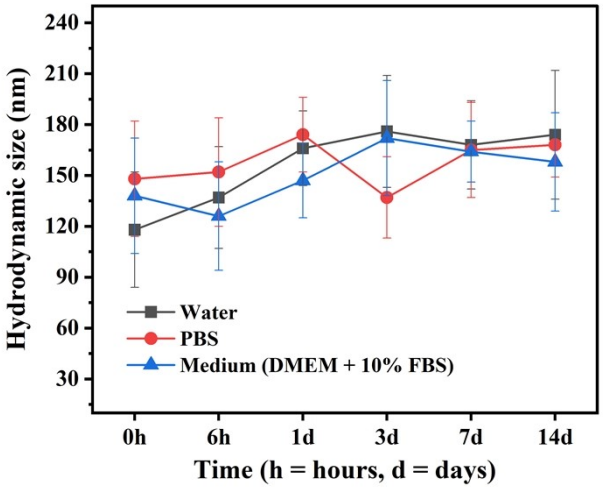

Figure S3. **Colloidal stability of f-MPNPs.** Colloidal stability was analyzed in water, PBS, and cell culture media (DMEM + 10% FBS). A known concentration of NPs was prepared in water, PBS, and DMEM media and stored at 25 °C. (n = 5 for each media) The hydrodynamic size was measured at predetermined time intervals for a 14-day study period.

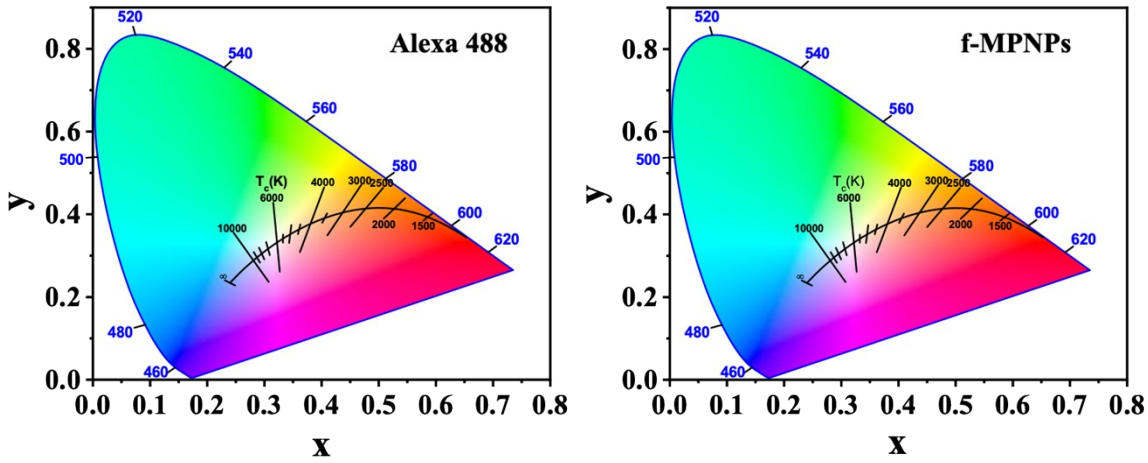

Figure S4. CIE fluorescent plot of fluorescent dye with and without conjugation; **(A)** Alexa Fluor 488 dye and **(B)** Alexa Fluor 488 conjugated MPNPs (f-MPNPs).

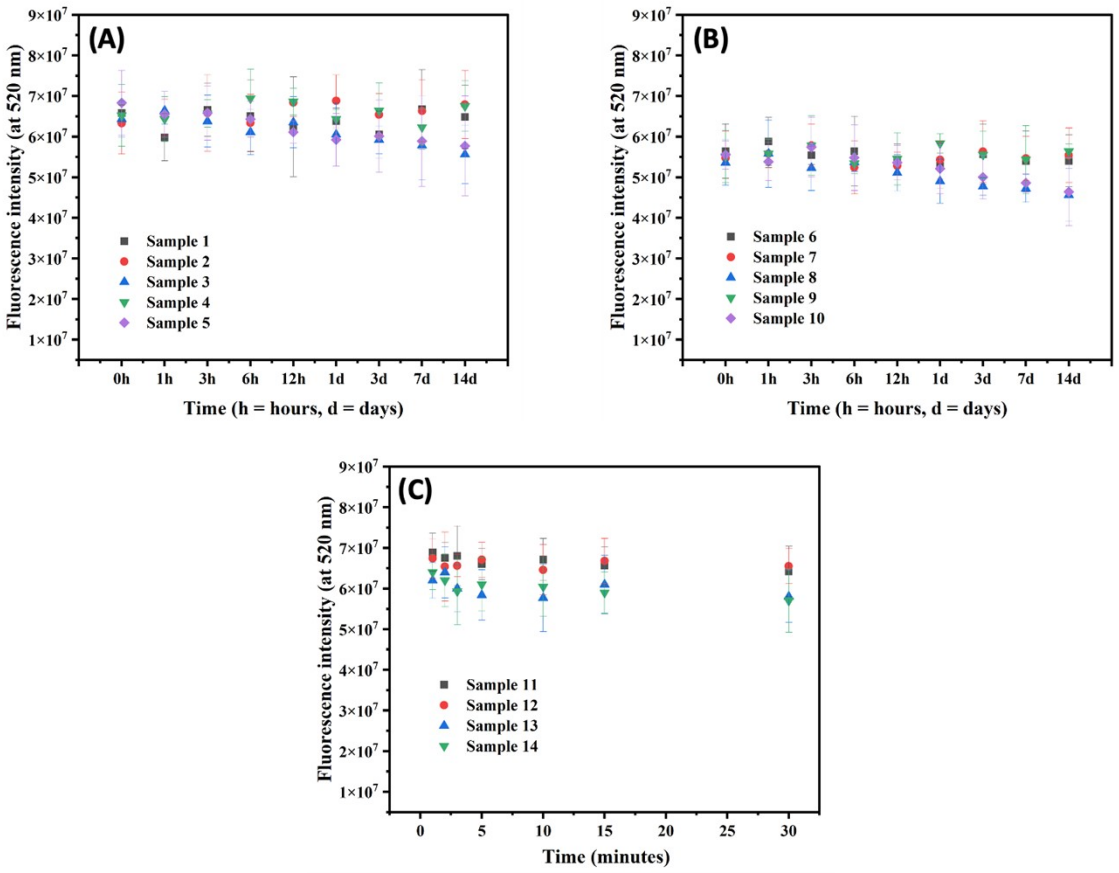

Figure S5. **Photostability of f-MPNPs.** The photostability of f-MPNPs was evaluated at different conditions. The samples were preconditioned at various conditions (**Solvent/Temperature/Light**) and then photostability tests were performed by recording the fluorescence emission at 520 nm by excitation at 488 nm wavelength. Two solvents were selected: PBS and rat blood plasma (Plasma). Three light conditions were applied: dark, bright light (daylight lamp) and illumination under LED light source of wavelength 488 nm. We selected three temperature conditions: 4°C (storage temperature), 25°C (room temperature) and 37°C (body temperature). **(A)** f-MPNPs were dissolved in PBS and different conditions were applied; **Sample 1 -** PBS/4°C/Dark; **Sample 2 -** PBS/25°C/Dark, **Sample 3 -** PBS/37°C/Dark, **Sample 4 -** PBS/25°C/Bright, and **Sample 5 -** PBS/37°C/Bright. **(B)** f-MPNPs were dissolved in plasma and different conditions were applied; **Sample 6 -** Plasma/4°C/Dark, **Sample 7 -** Plasma/25°C/Dark, **Sample 8 -** Plasma/37°C/Dark, **Sample 9 -** Plasma/25°C/Bright, and **Sample 10 -** Plasma/37°C/Bright. **(C)** f-MPNPs solutions were irradiated with 488 nm LED light for definite time: **Sample 11 -** PBS/25°C/LED, **Sample 12 -** PBS/37°C/LED, **Sample 13 -** Plasma/25°C/LED, and **Sample 14 -** Plasma/37°C/LED. (n = 5 for each sample)

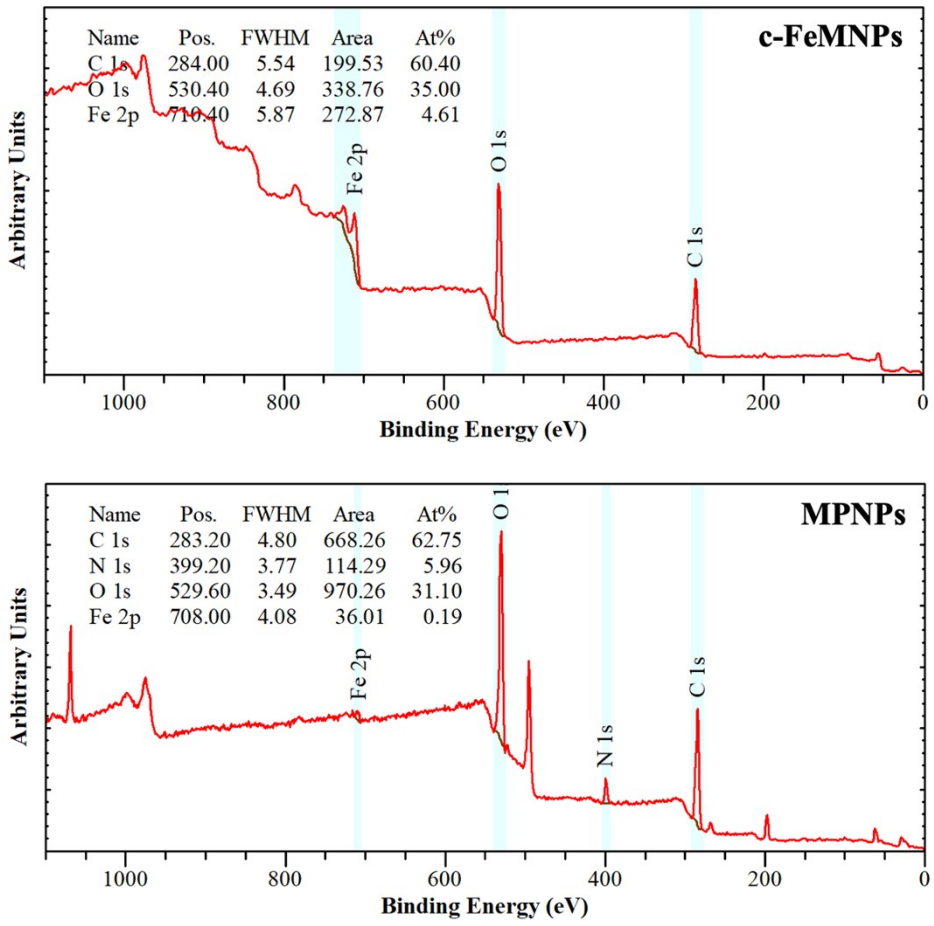

Figure S6. **XPS survey spectra of c-FeMNPs and MPNPs; (A)** c-FeMNPs, reveals elemental composition as C*1s*, O*1s* and Fe*2p*, and **(B)** MPNPs**,** reveals elemental composition as C*1s*, O*1s*, Fe*2p* and N*1s* peaks (some additional peaks denote Na and Cl elements from HCl, NaOH and saline solution).

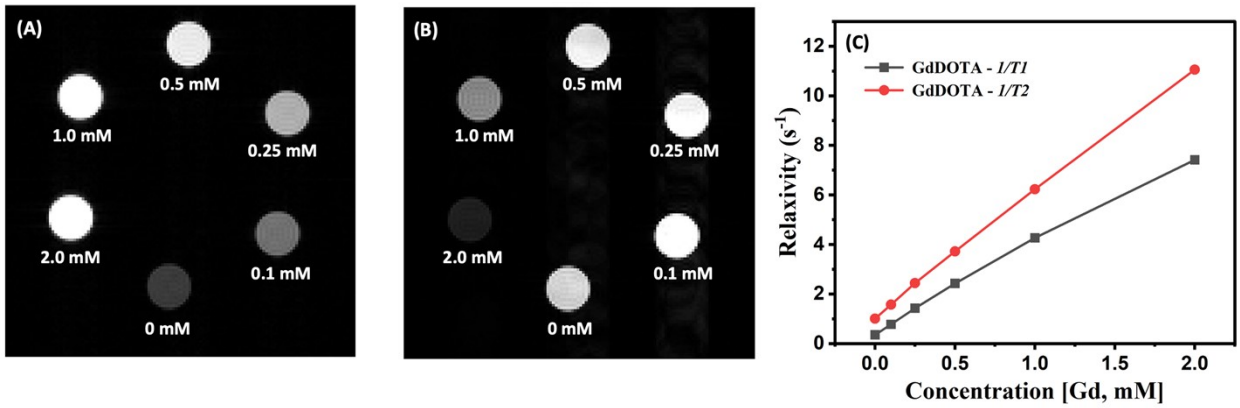

Figure S7. **Evaluation of MRI properties of GdDOTA. (A)** T1 weighted (*T1w*) **(B)** T2 weighted (*T2w*) images of GdDOTA for different Gd concentrations. **(C)** Relaxivity evaluation of Gd concentration; plots of GdDOTA; *1/T1* (black ■), *1/T2* (red ●). The slope indicates the specific relaxivity (r). The series of concentrations of GdDOTA reveals longitudinal relaxivity (r1) = 4.26, transverse relaxivity (r2) = 6.23, and the $r_2/ r_1 = 1.46$, at 11.7T.

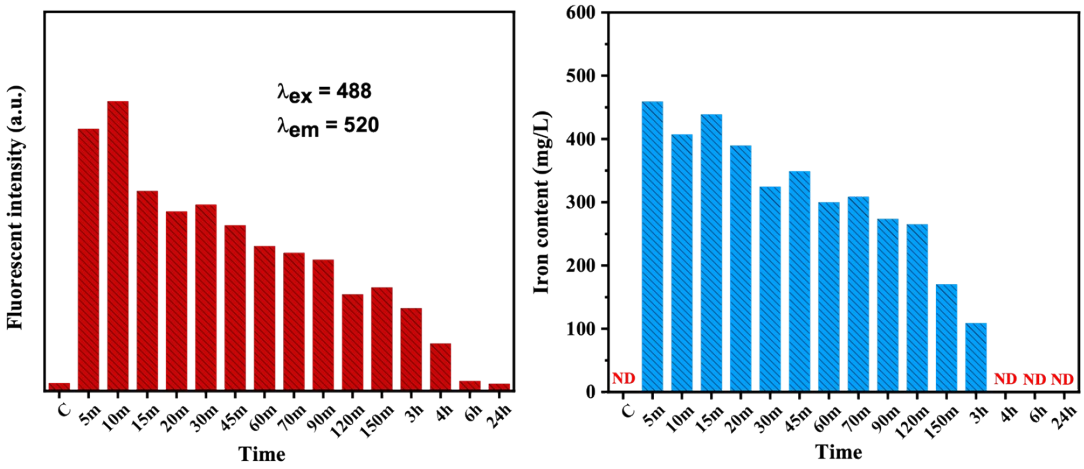

Figure S8. Blood half-life and iron content of MNPs. **(A)** Blood half-life of f-MPNPs estimated by measuring fluorescence intensity (λex = 488, λex = 520) by plate reader and **(B)** iron content in blood plasma by ICP-MS. Both methods reveal a circulation half-life of 90-100 minutes from rat blood samples.

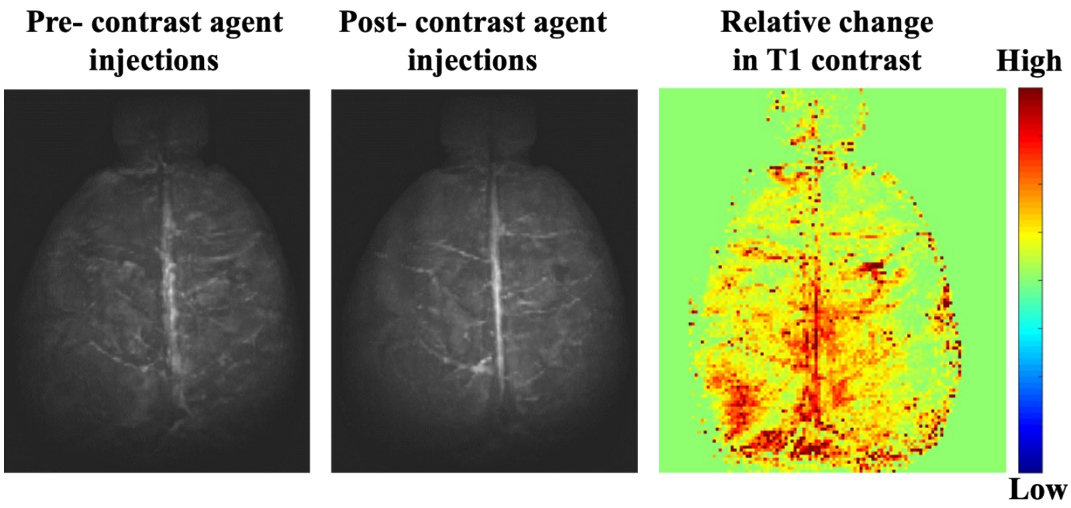

Figure S9. Cerebral angiography by real-time in vivo MRA of rats. Data from rat brain treated with f-MPNPs demonstrates enhanced 30-40% T1 contrast enhancement using 3D-FLASH sequence. (Scale = low to high represents 0 to 100 % arbitrary unit)

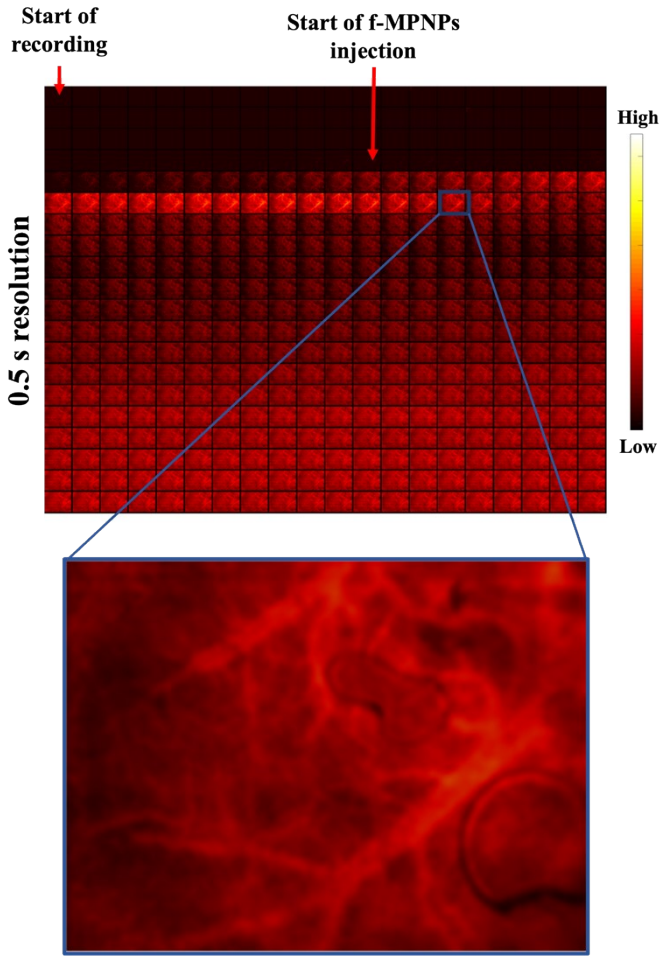

Figure S10. Cerebral angiography by real-time in vivo fluorescence imaging of rat brain after intravenously injection with f-MPNPs (image resolution = 0.5s). Scale = 1mm. (Scale = low to high represents 0 to 100 % arbitrary unit)

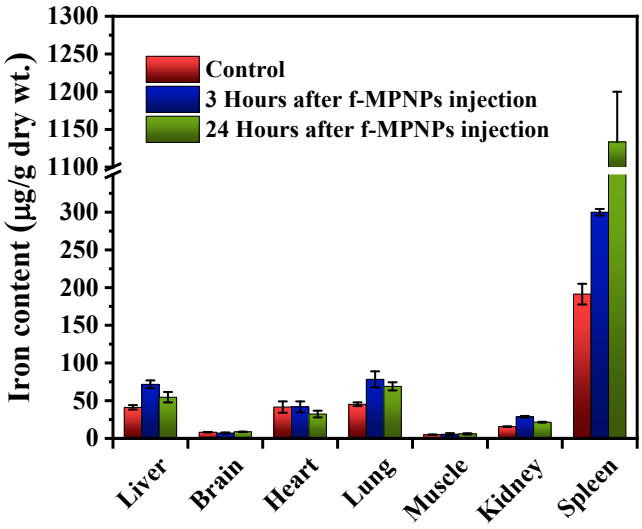

Figure S11. Biodistribution pattern for 3h and 24 h after intravenous injection of the f-MPNPs in rats.